SIGNAL ANALYSIS AND MODELING OF WIND TURBINE CLUTTER IN WEATHER RADARS

Kumar Vijay Mishra and V. Chandrasekar

Colorado State University, Fort Collins, CO

ABSTRACT

Lately, the continuing expansion of wind energy industry has led to the installation of several wind farms which are often in the vicinity of the weather radars. This is a source of growing concern for the weather radar community since wind turbines interfere with the normal operation of the weather radars. The wind turbine tower can drive the receivers into saturation and the Doppler shift from the moving blades can introduce errors in the estimation of wind speed, reflectivity and rainfall rates. The radar cross-section of the wind turbines has a large temporal and spatial variation which poses additional difficulties for traditional clutter filtering algorithms. This paper presents a first-order theoretical model of the radar signature of a wind turbine that can be helpful in deducing its unique features to be incorporated in filtering out the wind turbine clutter. A comparison with the observations from an S-band radar is made later in the paper.

Index Terms— wind turbine clutter, scattering, CSU-CHILL, rcs

1. INTRODUCTION

The production of wind energy has greatly accelerated around the world in the last few years as wind is a renewable and clean energy source. Global Wind Energy Council reports United States as the world′s largest wind-power producer in 2009 and the installed global wind power capacity to be more than 150 GW [1]. This boom in global wind power is accompanied by a surge in the installation of several wind farms often nearer to the weather radars as, in both the cases, secure and unpopulated sites are desired [2]. The wind farms have considerably larger radar cross-section and they can be easily detected by the weather radars [3]. Also, the size and height of the installed wind turbines is continously increasing [4] causing weather radars to be even more susceptible to wind turbine interference. The strong reflections from the wind tower structure can drive the radar receivers to saturation [3] and the echoes originating from the rotating blades (with tip velocities often exceeding unambiguous Doppler velocities) can affect the measurement of the wind speed, introduce errors in the estimation of the rainfall rates or even trigger false alarms for mesoscale weather phenomena [5]. There is, therefore, considerable interest in the problem of identifying and mitigating the clutter originating from the presence of wind energy farms. In this paper, we present a numerical model for theoretical analysis of the radar signature from a wind turbine based on the radar cross-section models. This model is then compared against the actual signal returns from a wind farm as observed by the S-band CSU-CHILL radar [6] and comments are made on the factors that influence this model.

This research was supported by the Colorado State University.

2. THEORETICAL MODEL OF WIND TURBINE SIGNATURE

A typical wind turbine consist of a tower, rotor blades and the nacelle which houses shafts, gear box and the generator. The offshore wind turbines also have different types of floating platform structures [7]. The geometrical dimensions of a wind turbine generator (WTG) vary a lot but typically the tower height is 40-120 m and the blade length is 10-40 m [4][8]. The number of blades is also variable though the common designs would usually have three considering the aerodynamic efficiency, load and cost [2][7]. The wind turbine towers act as large radar targets while the rotating wind blades represent moderate radar targets. The rotating wind turbine blades present a time -varying radar cross-section (RCS) affected by the rotational speed f_{rot} of the wind turbine generator.

Usually a wind turbine blade is composed of a hollow shell of fiberglass-reinforced polyester. In some models, within the dielectric shell of the blade, there may exist a conducting wire (with a diameter of few mm) for the purpose of lightning protection. To model the radar return from a WTG, each blade can be assumed to be a cylinder of length L. It is possible that based on the transmit frequency of the radar, either the dielectric or the conducting part of the blade dominates the signature. Further, for radars operating in the S-band, the scattering regime for the lightning wire is optical. It has also been argued [9] that traditional RCS scheme is not applicable for the ground-based objects like wind turbines, however a first-order RCS model of a wind turbine can be useful in determining unique features that are associated with the wind turbine echo. The RCS of a single WTG can be

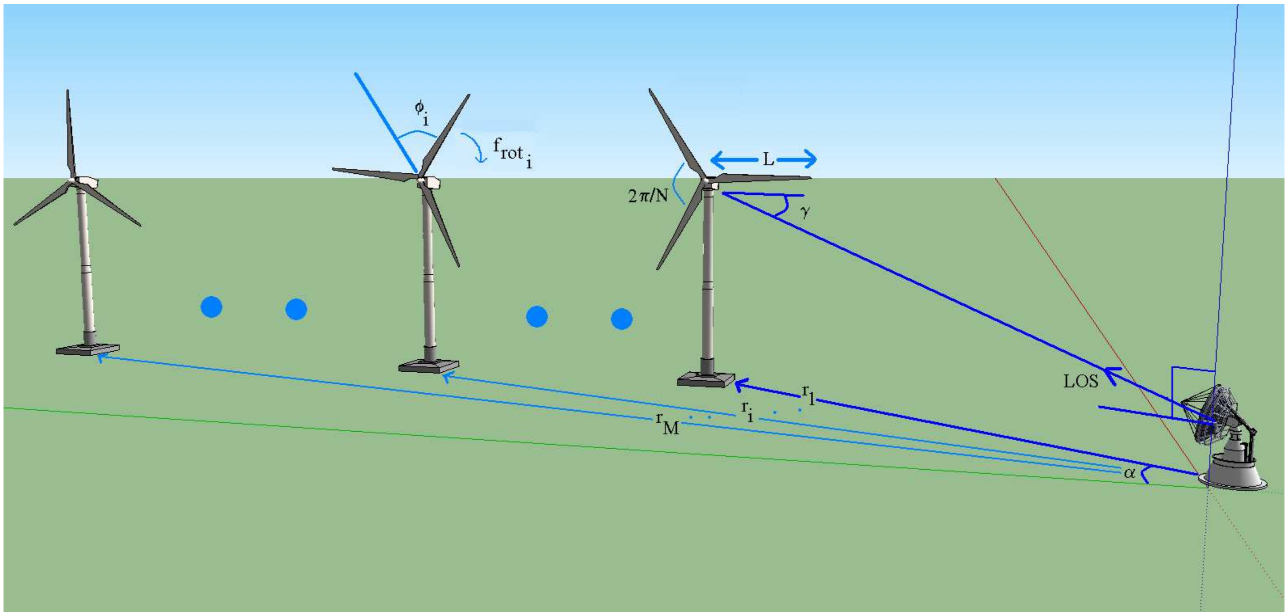

Fig. 1. Geometry of the wind turbine for numerical modeling of the radar return. N is the number of blades per WTG, f_{roti} is the rotation speed of the i^{th} WTG in the resolution cell, r_i is the range at which the tower of i^{th} WTG is situated with respect to the radar.

formulated by modifying the RCS models of the conducting or dielectric cylinder [10][11] such that it also incorporates the number of blades, rotational speed and dimensions of the wind turbine as follows:

Highly conducting thin cylinder assumption -

$$\sigma(t) = \sum_{n=1}^{N} \frac{\pi L^2 \sin^2\theta \mathrm{sinc}^2\delta}{(\ln(ka/2) + 0.5772)^2} \tag{1}$$

Thin dielectric cylinder assumption -

$$\sigma(t) = \sum_{n=1}^{N} \frac{\pi L^2 (ka)^4 (\eta^2 - 1)^2 \sin^2\theta \mathrm{sinc}^2\delta}{4} \tag{2}$$

where
$\theta = (2\pi f_{rot}t + (2\pi(n-1)/N))$,
$\delta = (kL/2)\cos(2\pi f_{rot}t + (2\pi(n-1)/N))$,
N = total number of rotor blades in the WTG,
f_{rot} = frequency of blade rotation of the WTG (rpm),
L = length of the turbine blade (m),
a = radius of the cylinder (m),
$k = 2\pi/\lambda$ where λ = radar wavelength (m)
η = Refractive index of the dielectric (≈ 2.7 for solid fibreglass) [10].

The above assumes that the plane of rotation of the wind turbine blades is same as the line of sight of the observing radar. However, in general, this may not be the case. Assuming that the elevation of the WTG with respect to the radar is γ (radians) and the angle between the radar's LOS and the rotation plane of WTG is α (radians) (Figure 1), the required transformation in the models above will be $L \rightarrow L\cos(\alpha)\cos(\gamma)$.

The backscatter from the wind farm is usually more complicated than the return from a single wind turbine. Depending on the range and beam resolution of the radar and the layout of the wind farm, it is possible that the return consists of echos from more than one WTG. These WTGs may all be of different dimensions and rotating at different speed with relative phase-shifts to each other (Figure 1). In such a case, based on either (1) or (2), the time-varying return signal S(t) from one or more WTGs in the same resolution cell can be formulated as

$$S(t) = A \sum_{i=1}^{M} \sum_{n=N_i}^{N} L_i \cos(\alpha)\cos(\gamma)\sin(\theta_i)\mathrm{sinc}(\delta_i) e^{-j(4\pi r_i/\lambda)} \tag{3}$$

where
$\theta_i = 2\pi f_{rot_i}t + (2\pi(n-1)/N_i) + \phi_i$,
$\delta_i = (kL_i/2)\cos(\alpha)\cos(\beta)\cos(2\pi f_{rot_i}t + (2\pi(n-1)/N))$,
N_i = total number of rotor blades in the i^{th} WTG,
f_{rot_i} = frequency of blade rotation of the i^{th} WTG (rpm),
L_i = length of the rotor blade of i^{th} WTG (m),
M = number of WTGs in the resolution cell,
ϕ_i = relative phase shift of i^{th} WTG with respect to a refernce WTG (Figure 1),
r_i = Range of i^{th} WTG from the radar,

A = scale factor.

The above model can be further generalized to include the beampattern of the radar antenna, varying heights of each wind turbine in a resolution cell, the relative orientation of individual blades for the wind turbines with pitching-blades and receiver noise.

3. COMPARISON WITH THE OBSERVATIONS FROM AN S-BAND RADAR

The theoretical model described above was used to simulate returns from the Ponnequin Wind Farm located in the Weld County of the US state of Colorado. The CSU-CHILL S-band radar (at Greeley: 40.44625 N, 104.63708 W, 1426 m altitude) was used to record radar return from wind turbines at Ponnequin Wind Farm, Colorado. The wind farm is located at a range of approximately 62-63 km at azimuth 344-347 from the radar (Figure 2). Figure 3 shows the layout and location of individual wind turbines of Ponnequin Wind Farm with respect to the CSU-CHILL radar. This plant consists of 44 installed wind turbines of which 29 are NEG Micon (N01-N29) and the rest (V01-V15) are Vestas models. Radar echoes were recorded from the wind turbines on Aug 15, 2008 at 150m range resolution and a pulse repetition frequency of 957 Hz. Figure 4 shows the time and spectral plots of the radar return at a range of 63.15 km, 345.5 azimuth and 0.35 elevation. The observation was made at a fixed antenna position (spotlight mode). Since the maximum return occurs when the wind turbine blades are perpendicular to the line of sight, the time domain return consists of large reflection flashes. The frequency of these flashes is obviously a function of the number of blades per wind turbine and its rotation speed. From this, an approximate value of rpm can be deduced which in this case can be in the range 10-20 rpm. The maximum Doppler frequency due to return from a wind turbine can be calculated as $f_{max} = 2v_{max}/\lambda$ where the maximum radial velocity v_{max} = L$(2\pi/60)f_{rot}$.

A close examination of the exact locations of the individual wind turbines indicate that the observed data should be the return from N10 and may also possibly include return from one of the adjacent wind turbines. The NEG Micon wind turbines installed in the plant have a tower height of 55 m and rotor diameter of 48.2 m. The relative orientation of the rotation plane of N10 can be estimated to be only slightly off the line of sight based on the available satellite pictures around the observation date mentioned above. Using this information, the available specifications and locations of the particular wind turbines of Ponnequin Wind Farm, the theoretical return based on the model described in the previous section is simulated as shown in Figure 5. It should be noted that it reasonably mimics the observed return.

Various parameters related to the geometry of the wind turbines considerably influence the radar return. The rotation speed of the wind turbines is directly related to the Doppler

Fig. 2. Location of the Ponnequin Wind Farm with respect to the CSU-CHILL radar (Source: Google Earth)

spread of the signal for a fixed sampling frequency of the radar. The NEG Micon wind turbines have fixed rotation speed of 14 or 20 rpm depending on the wind load. The estimate from the observed spectra indicates the rotation speed to be between 10-20 rpm. The rotation of the blade is however much complex and, in general, different points of the rotor blade have different radial speeds associated with them. Also, the wind speeds that drive each wind turbine are also affected by the farm's layout (crosswind and downwind spacing) giving rise to the spatio-temporal variation of the wind speed within the wind farm. The length of the rotor blade determines the centre notch between the sidebands in the spectra. Another important factor which affects both the strength of the return as well as its Doppler spread is the angle between the line-of-sight and the rotation plane of the wind turbine. This is also one of the reasons why a strong echo is not observed for all the wind turbines in the same wind farm for they may be aligned differently with respect to the line-of-sight. The echo is strongest when the LOS and wind turbine's rotation plane are co-aligned and as the rotation plane moves away from the LOS, the strength drops considerably.

4. CONCLUSIONS

This study presents a preliminary analysis of the wind turbine signals as seen by the weather radars. Several parameters associated with the wind turbine geometry as well as the observing radar influence the nature of wind turbine echo. The RCS-based model can only account for the first-order effects associated with the backscatter but is useful in characterizing the return. In the future, this model is intended to study the signal from wind turbines when overlaid precipitation, in order to develop the techniques for identification and mitigation of wind turbine clutter.

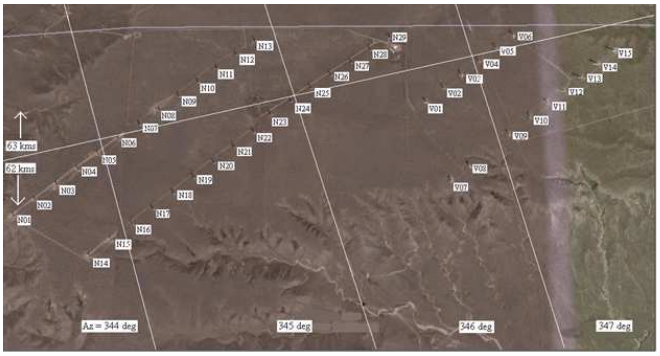

Fig. 3. Layout of the Ponnequin wind farm showing the individual wind turbines. The relative range and azimuth with respect to the CSU-CHILL radar are boradly marked (Source: Google Earth).

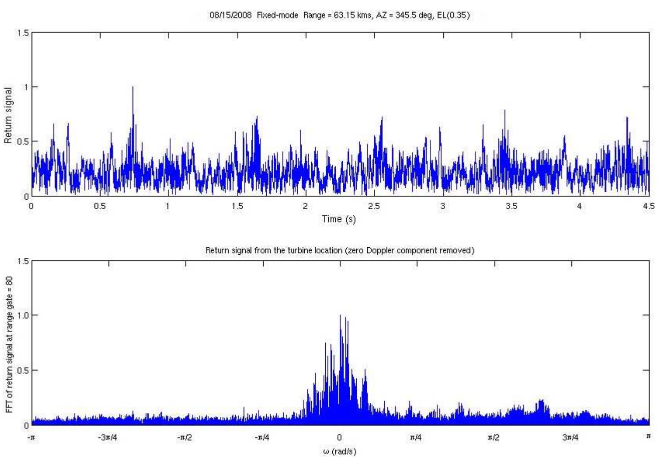

Fig. 4. Time (top) and spectral (bottom) plots of the return from a WTG situated in the Ponnequin wind farm as observed by the CSU-CHILL radar on Aug 15, 2008.

5. ACKNOWLEDGEMENT

The authors would like to acknowledge the Colorado State University CHILL facility for obtaining the data used in this work.

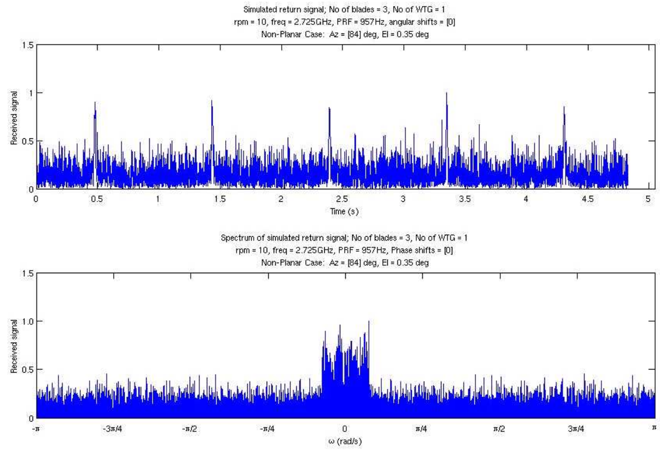

Fig. 5. Simulated time (top) and spectral (bottom) plots for a noisy return from a single wind turbine for a non-planar case. The length of the rotor blade is assumed to be 24 m and rpm = 10.

6. REFERENCES

[1] S. Sawyer and A. Zervos, "Global wind 2009 report," Global Wind Energy Council, Brussels, Belgium, Tech. Rep., 2009.

[2] N. P. Cheremisinoff, *Fundamentals of Wind Energy*. Ann Arbor Science Publishers Inc, 1978.

[3] G. J. Poupart, "Wind farms impact on radar aviation interests final report," QinetiQ Ltd, Worcestershire, Tech. Rep., 2009.

[4] M. L. Fossdal, E. Arnstad, K. B. Mathiesen, and B. Eriksen, "Renewable energy," www.renewableenergy.no, Tech. Rep., 2007.

[5] R. J. Vogt, J. R. Reed, and T. Crum, "Impacts of wind farms on WSR-88D operations and policy considerations," in *Proc. 23rd Conference on IIPS*, no. paper 6B.4, January 2007.

[6] V. N. Bringi and V. Chandrasekar, *Polarimetric Doppler Weather Radar: Principles and Applications*. Cambridge University Press, 2001.

[7] L. Y. Pao and K. E. Johnson, "A tutorial on the dynamics and control of wind turbines and wind farms," in *Proc. American Control Conf.*, St. Louis, MO, June 2009, pp. 2076–2089.

[8] (2009) Wind turbine models. Vestas Wind Systems. [Online]. Available: http://www.vestas.com/en/wind-power-solutions/wind-turbines.aspx

[9] G. Greving and M. Malkomes, "Weather radar and wind turbines - theoretical and numerical analysis of the shadowing effects and mitigation concepts," in *ERAD 2008 5th European Conference on Radar in Meteorology and Hydrology*, Helsinki, Finland, 2008.

[10] R. J. Riddolls, "Effects of wind turbines on high frequency surface radar," Defence R&D Canada, Ottawa, Tech. Rep., 2005.

[11] P. Z. Peebles, *Radar Principles*. Wiley Interscience, 1998.